

Scheduling Links for Heavy Traffic on Interfering Routes in Wireless Mesh Networks

Fabio R. J. Vieira^{1,2,*}
 José F. de Rezende³
 Valmir C. Barbosa¹
 Serge Fdida²

¹Programa de Engenharia de Sistemas e Computação, COPPE
 Universidade Federal do Rio de Janeiro
 Caixa Postal 68511, 21941-972 Rio de Janeiro - RJ, Brazil
²Laboratoire d'Informatique de Paris 6
 4, Place Jussieu, 75252 Paris Cedex 05, France
³Programa de Engenharia Elétrica, COPPE
 Universidade Federal do Rio de Janeiro
 Caixa Postal 68504, 21941-972 Rio de Janeiro - RJ, Brazil

Abstract

We consider wireless mesh networks and the problem of scheduling the links of a given set of routes under the assumption of a heavy-traffic pattern. We assume some TDMA protocol provides a background of synchronized time slots and seek to schedule the routes' links to maximize the number of packets that get delivered to their destinations per time slot. Our approach is to construct an undirected graph G and to heuristically obtain node multicolorings for G that can be turned into efficient link schedules. In G each node represents a link to be scheduled and the edges are set up to represent every possible interference for any given set of interference assumptions. We present two multicoloring-based heuristics and study their performance through extensive simulations. One of the two heuristics is based on relaxing the notion of a node multicoloring by dynamically exploiting the availability of communication opportunities that would otherwise be wasted. We have found that, as a consequence, its performance is significantly superior to the other's.

Keywords: Wireless mesh networks, Link scheduling, Node multicolorings, Scheduling by edge reversal.

*Corresponding author (fjimenex@cos.ufrj.br).

1 Introduction

Owing to their numerous advantages, wireless mesh networks (WMNs) constitute a promising solution for community networks and for providing last-mile connections to Internet users [1, 3, 22]. However, like all wireless networks WMNs suffer from the problem of decreased capacity as they become denser, since in this case attempting simultaneous transmissions causes interference to increase significantly [15, 25]. One common solution to reduce interference is to adopt some contention-free TDMA protocol [11] and schedule simultaneous transmissions for activation only if they do not interfere with one another. Doing this while maximizing some measure of network usage and guaranteeing that all links are given a fair treatment normally translates into a complicated optimization problem, one that unfortunately is NP-hard [4].

This scheduling problem has been formulated in a great variety of manners and has received considerable attention in the literature. Prominent studies include some that seek to calculate the capacity of the network [15, 13], others whose goal is the study of the time complexity associated with the resulting schedules [21], and still others that aim at scheduling transmissions in order to achieve as much of the network's capacity as possible [10, 2, 28, 12, 16, 27, 23, 30, 29]. One common thread through most the latter is that, having adopted a graph representation of the network and of how the various transmissions can interfere with one another, a solution is sought through some form of graph coloring. More often than not the transmissions to be scheduled are represented by the graph's nodes and then node coloring, through the abstraction of an independent set to represent the transmissions that can take place simultaneously, is used. But sometimes it is the graph's edges that stand for transmissions, in which case edge coloring is used, building on the abstraction of matchings to represent simultaneity [9].

Here we consider a variation of the problem which, to the best of our knowledge, is novel both in its formulation and in the solution type we propose. We start by assuming a WMN comprising single-channel, single-radio nodes and for which a set of origin-to-destination routes has already been determined, and consider the following question. Should there be an infinite supply of packets at each origin to be delivered to the corresponding destination in the FIFO order, and should all nodes in the network be endowed with only a finite number of buffers for the temporary storage of in-transit packets, how can transmissions be scheduled to maximize the number of packets that get delivered to the destinations per TDMA slot without ever stalling a transmission, by lack of buffering space, whenever it is scheduled? This question addresses issues that lie at the core of successfully designing WMNs and their routing protocols, since it seeks to tackle the problem of transmission interference when the network is maximally strained. The solution we propose is, like in so many of the approaches mentioned above, based on coloring a graph's nodes. Unlike them, however, we use node multicolorings instead [26], which are more general and for this reason allow for a more suitable formulation of the optimization problem to be solved.

Given the origin-to-destination routes (or paths) to be used, we begin in Section 2 with a precise definition of a schedule and a precise formulation of the problem. We also show, through an example, that had the problem been formulated for network-capacity maximization, a conflict with the requirement of finite buffering might arise. Then we move, in Section 3, to the specification of the undirected graph that underlies our algorithm's operation. One assumption in that section, and therefore throughout most of the paper, is that the communication and interference radii are the same for the WMN at hand. Moreover, we also assume that the tenets of the protocol-based interference model [8, 24], including the possibility of bidirectional communication in each transmission, are in effect. In Section 4 we guide the reader through various multicoloring possibilities, which culminates in Section 5 with a preliminary method for scheduling, borrowed from the field of resource sharing [5]. Improving on this preliminary method with the goals of the problem formulated in Section 2 in mind finally yields our proposal in Section 6. This proposal, essentially, stems from a slight relaxation of the notion of a node multicoloring. The subsequent two sections are dedicated to the presentation of computational results, with the methodology laid down in Section 7 and the results proper in Section 8. Discussion follows in Section 9 and we close in Section 10.

2 Problem formulation

We consider a collection $\mathcal{P}_1, \mathcal{P}_2, \dots, \mathcal{P}_P$ of simple directed paths (i.e., directed paths that visit no node twice), each having at least two nodes (a source and a destination). These paths' sets of nodes are X_1, X_2, \dots, X_P , respectively, not necessarily disjoint from one another, and we let $X = \bigcup_{p=1}^P X_p$. Their sets of edges are Y_1, Y_2, \dots, Y_P and we assume that, for $p \neq q$, a member of Y_p and one of Y_q are distinguishable from each other even if they join the same two nodes in the same direction. Letting $Y = \bigcup_{p=1}^P Y_p$, we then see that Y may contain more than one edge joining the same two nodes in the same direction (parallel edges) or in opposing directions (antiparallel edges).

Our discussion begins with the definition of the directed multigraph $D = (X, Y)$, where all P directed paths are represented without sharing any directed edges among them. An example is shown in Figure 1. We take D to be representative of a wireless network operating under some TDMA protocol. In this network, each of paths $\mathcal{P}_1, \mathcal{P}_2, \dots, \mathcal{P}_P$ is to transmit an unbounded sequence of packets from its source to its destination. Such transmissions are to occur without contention, meaning that whenever an edge is scheduled to transmit in a given time slot no other edge that can possibly interfere with that transmission is to be scheduled at the same time slot. We assume that each transmission sends at most one packet across the edge in question (more specifically, it sends exactly one packet if there is at least one to be sent but does nothing otherwise). We also assume that each transmission may involve the need for bidirectional communication for error control.

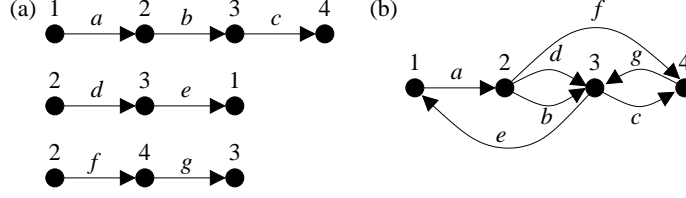


Figure 1: A set of $P = 3$ directed paths (a) and the resulting directed multigraph D (b).

We call a schedule any finite sequence $\mathcal{S} = \langle S_0, S_1, \dots, S_{L-1} \rangle$ such that $S_\ell \subseteq Y$ for $0 \leq \ell \leq L-1$, provided $\bigcup_{\ell=0}^{L-1} S_\ell = Y$ and moreover no two concurrent transmissions on edges of the same S_ℓ can interfere with each other. To schedule the transmissions according to \mathcal{S} is to cycle through the edge sets S_0, S_1, \dots, S_{L-1} , indefinitely and in this order, letting all edges in the same set transmit in the same time slot whenever that set is reached along the cycling. Given \mathcal{S} , we let $\text{length}(\mathcal{S}) = L$ and denote by $\text{delivered}(\mathcal{S})$ the number of packets that can get delivered to all paths' destinations during a single repetition of \mathcal{S} in the long run (i.e., in the limit as the number of repetitions grows without bound). Of course, $\text{delivered}(\mathcal{S})$ is bounded from above by the number of times the P paths' terminal edges (those leading directly to a destination node) appear in \mathcal{S} altogether.

Before we use these two quantities to define the optimization problem of finding a suitable schedule for D , we must recognize that our focus on the source-to-destination packet flows on the paths $\mathcal{P}_1, \mathcal{P}_2, \dots, \mathcal{P}_P$ carries with it the inherent constraint that the nodes' capacity to buffer in-transit packets cannot be allowed to grow unbounded. We then adopt an upper bound B on the number of in-transit packets that a node can store for each of the paths (at most P) that go through it. However, there is still a decision to be made regarding the effect of such a bound on the transmission of packets. One possibility would be to impose that, when it is an edge's turn to transmit it does so if and only if there is a packet to transmit and, moreover, there is room to store that packet if it is received as an in-transit packet. Another possibility, one that seeks to never stall a transmission by lack of a buffer to store the packet at the next intermediate node, is to only admit schedules that automatically rule out the occurrence of such a transmission. We adopt the latter alternative.

The following, then, is how we formulate our scheduling problem on D . Find a schedule \mathcal{S} that maximizes the throughput

$$T(\mathcal{S}) = \frac{\text{delivered}(\mathcal{S})}{\text{length}(\mathcal{S})}, \quad (1)$$

subject to the following two constraints:

- C1. Every node can store up to B in-transit packets for each of the source-to-destination paths that go through it.

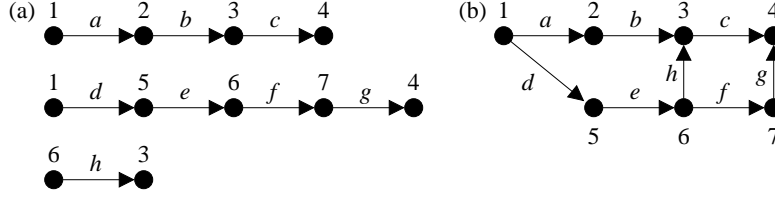


Figure 2: A set of $P = 3$ directed paths (a) and the resulting directed multigraph D (b). Using the schedule \mathcal{S} such that $S_0 = \{a, f\}$, $S_1 = \{c, d\}$, $S_2 = \{b\}$, $S_3 = \{e\}$, $S_4 = \{a, g\}$, and $S_5 = \{h\}$ causes unbounded packet accumulation at node 2 when constraint C2 is in effect, thus violating constraint C1. Enforcing constraint C1 for some value of B causes constraint C2 to be violated.

- C2. Whenever an edge is scheduled for transmission in a time slot and a packet is available to be transmitted, if the edge is not the last one on its source-to-destination path then there has to be room for the packet to be stored after it is transmitted.

2.1 Scheduling for maximum network usage

Before proceeding, recall that, as mentioned in Section 1, the most commonly solved problem regarding the selection of a schedule \mathcal{S} is not the one we just posed, but rather the problem of maximizing network usage. In terms of our notation, this problem requires that we find a schedule that maximizes

$$U(\mathcal{S}) = \frac{\sum_{\ell=0}^{L-1} |S_\ell|}{\text{length}(\mathcal{S})} \quad (2)$$

without any constraints other than those that already participate in the definition of a schedule.

It is a simple matter to verify that solutions to this problem often fail to respect constraints C1 and C2 of our formulation. This is exemplified in Figure 2.

3 Graph transformation

We wish to address the problem of optimizing $T(\mathcal{S})$ exclusively in terms of some underlying graph. Clearly, though, the directed multigraph D is not a good candidate for this, since it does not embody any representation of how concurrent transmissions on its edges can interfere with one another. Our first step is then to transform D into some more suitable entity, which will be the undirected graph $G = (N, E)$ defined as follows:

1. The node set N of G is the edge set Y of D . In other words, G has a node for every edge of D . Since D is a multigraph, a same pair of nodes $i, j \in X$ such that $(i, j) \in Y$ or $(j, i) \in Y$ may appear more than once as a member of N .

2. The edge set E of G is obtained along the following four steps:
 - i. Enlarge N by including in it all node pairs of D that do not correspond to edges on any of the P source-to-destination paths but nevertheless reflect that each node in the pair is within the interference radius of the other. We refer to these extra members of N as temporary nodes.
 - ii. Connect any two nodes in N by an edge if, when regarded as node pairs from D , they share at least one of the nodes of D . In other words, if each of the two pairs $i, j \in X$ and $k, l \in X$ corresponds to a node of G (by virtue of either constituting an edge of D or being a temporary node), then the two get connected by an edge in G if at least one of $i = k$, $i = l$, $j = k$, or $j = l$ holds.
 - iii. Connect any two nodes in N by an edge if, after the previous steps, the distance between them is 2.
 - iv. Eliminate all temporary nodes from N and all edges from E that touch them.

Together, these four steps amount to using G to represent every possible interference that may arise under the assumptions of the protocol-based model when communication is bidirectional. Graph G is also known as a distance-2 graph relative to D [4]. The entire transformation process, from the set of P paths through graph G , is illustrated in Figure 3.

It follows from this definition of G that any group of nodes corresponding to parallel or antiparallel edges in D are a clique (a completely connected subgraph) of G . Similarly, every group of three consecutive edges on any of the paths $\mathcal{P}_1, \mathcal{P}_2, \dots, \mathcal{P}_P$ corresponds to a three-node clique in G . As we discuss in Section 9, these and other cliques are related to how large $T(\mathcal{S})$ can be under one of the scheduling methods we introduce.

It is also worth noting that Steps 1 and 2 above are easily adaptable to modifications in any of the assumptions we made. These include the assumptions that the communication and interference radii are the same and that communication is bidirectional. Changing assumptions would simply require us to adapt Steps 2.i through 2.iii accordingly.

4 Multicoloring-based schedules

Graph G allows us to rephrase the definition of a schedule as follows. We call a schedule any finite sequence $\mathcal{S} = \langle S_0, S_1, \dots, S_{L-1} \rangle$ such that $S_\ell \subseteq N$ for $0 \leq \ell \leq L-1$, provided $\bigcup_{\ell=0}^{L-1} S_\ell = N$ and moreover every S_ℓ is an independent set of G . The appearance of the notion of an independent set in this definition leads the way to a special class of schedules, namely those that can be identified with graph multicolorings [26].

For $q \geq 1$, a q -coloring of the nodes of G is a mapping from N , the graph's set of nodes, to \mathbb{N}^q , where \mathbb{N} is the set of natural numbers, such that no two of a

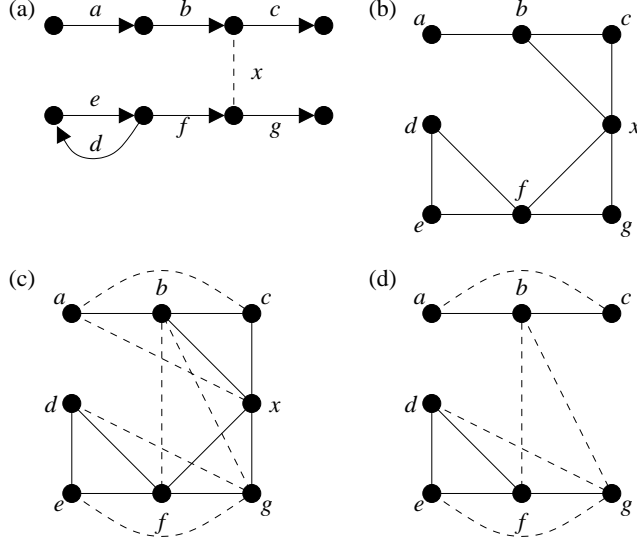


Figure 3: The graph-transformation process. We start with the directed multi-graph D (a), to which the node pair labeled x is added as a dashed line to indicate the existence of interference that is not internal to any of the initial P paths. Panel (b) contains the undirected graph G as it stands after Step 2.ii. Panels (c) and (d) show G past Steps 2.iii and 2.iv, respectively. In these two panels, dashed lines are used to represent the edges added in Step 2.iii.

node's q colors are the same and besides none of them coincides with any one of any neighbor's q colors. Of course, the set of nodes receiving one particular color is an independent set. If p is the total number of colors needed to provide G with a q -coloring, then N is covered by the p independent sets that correspond to colors and every node is a member of exactly q of these sets. Therefore, letting $L = p$ and identifying each S_ℓ with the set of nodes receiving color ℓ implies that to every q -coloring of the nodes of G there corresponds a schedule \mathcal{S} .

These multicoloring-derived schedules constitute a special case in the sense that every node of G can be found in exactly the same number of sets (q) out of the L sets that make up the schedule. Clearly, though, there are schedules that do not correspond to multicolorings. For now we concentrate on those that do and note that $\text{delivered}(\mathcal{S}) \leq Pq$ always holds (recall that P stands for the number of origin-to-destination paths). That is, the greatest number of packets that the P terminal edges of D can deliver during the L time slots of schedule \mathcal{S} is q per terminal edge. These schedules can be further specialized, as follows.

4.1 Standard coloring

When $q = 1$ every node of G receives exactly one color and $\text{length}(\mathcal{S}) = L \geq \chi(G)$, where $\chi(G)$ is the least number of colors with which it is possible to provide G with a 1-coloring, known as the chromatic number of G . Using $T^1(\mathcal{S})$ to denote $T(\mathcal{S})$ in this case, we have

$$T^1(\mathcal{S}) \leq \frac{P}{\chi(G)}. \quad (3)$$

4.2 Standard multicoloring

Coloring G 's nodes optimally in the previous case is minimizing the overall number of colors. This stems not only from the fact that $q = 1$, but more generally from the fact that q is fixed. We can then generalize and define $\chi^q(G)$ to be the least number of colors with which it is possible to provide G with a q -coloring. Evidently, $\chi(G) = \chi^1(G) < \chi^2(G) < \dots$, so the question of multicoloring G 's nodes optimally when q is not fixed can no longer be viewed as that of minimizing the overall number of colors needed (as this would readily lead to $q = 1$ and $\chi(G)$ colors). Instead, we look at how efficiently the overall number of colors is used, i.e., at what the value of q has to be so that $\chi^q(G)/q$ is minimized. This gives rise to the multichromatic number of G , denoted by $\chi^*(G)$ and given by $\chi^*(G) = \inf_{q \geq 1} \chi^q(G)/q$. Because this infimum can be shown to be always attained, we use minimum instead and let q^* be the value of q for which $\chi^*(G) = \chi^{q^*}(G)/q^*$.

Using a q -coloring for scheduling amounts to having $\text{length}(\mathcal{S}) = L \geq \chi^q(G)$. In this case, letting $T^*(\mathcal{S})$ stand for $T(\mathcal{S})$ yields

$$T^*(\mathcal{S}) \leq \frac{Pq}{\chi^q(G)} \leq \frac{Pq^*}{\chi^{q^*}(G)} = \frac{P}{\chi^*(G)}. \quad (4)$$

4.3 Interleaved multicoloring

A special class of q -colorings is what we call interleaved q -colorings [7, 6, 31]. If i and j are two neighboring nodes of G , let $c_1^i < c_2^i < \dots < c_q^i$ be the q colors assigned to node i by some q -coloring, and likewise let $c_1^j < c_2^j < \dots < c_q^j$ be those of node j . We say that this q -coloring is interleaved if and only if either $c_1^i < c_1^j < c_2^i < c_2^j < \dots < c_q^i < c_q^j$ or $c_1^j < c_1^i < c_2^j < c_2^i < \dots < c_q^j < c_q^i$ for all neighbors i and j . If we restrict ourselves to interleaved q -colorings, then similarly to what we did above we use $\chi_{\text{int}}^q(G)$ to denote the least number of colors with which it is possible to provide G with an interleaved q -coloring, and similarly define the interleaved multichromatic number of G , denoted by $\chi_{\text{int}}^*(G)$, to be $\chi_{\text{int}}^*(G) = \inf_{q \geq 1} \chi_{\text{int}}^q(G)/q$. Once again it is always possible to attain the infimum, so we may take q^* to be the value of q for which $\chi_{\text{int}}^*(G) = \chi_{\text{int}}^{q^*}(G)/q^*$.

As for scheduling based on an interleaved q -coloring, it corresponds to having $\text{length}(\mathcal{S}) = L \geq \chi_{\text{int}}^q(G)$. As before, we use $T_{\text{int}}^*(\mathcal{S})$ in lieu of $T(\mathcal{S})$ and obtain

$$T_{\text{int}}^*(\mathcal{S}) \leq \frac{Pq}{\chi_{\text{int}}^q(G)} \leq \frac{Pq^*}{\chi_{\text{int}}^{q^*}(G)} = \frac{P}{\chi_{\text{int}}^*(G)}. \quad (5)$$

4.4 Discussion

It is a well-known fact that

$$\frac{1}{\chi(G)} \leq \frac{1}{\chi_{\text{int}}^*(G)} \leq \frac{1}{\chi^*(G)}. \quad (6)$$

The first inequality follows from the definition of $\chi_{\text{int}}^*(G)$, considering that every 1-coloring is (trivially) interleaved. As for the second inequality, it follows directly from the definition of $\chi^*(G)$. By these inequalities, should all of Eqs. (3)–(5) hold with equalities, we would have

$$T^1(\mathcal{S}) \leq T_{\text{int}}^*(\mathcal{S}) \leq T^*(\mathcal{S}). \quad (7)$$

Obtaining equalities in Eqs. (3)–(5), however, requires both that $\text{delivered}(\mathcal{S}) = Pq$ for $q = 1$ or $q = q^*$, as the case may be, and that $\text{length}(\mathcal{S}) = \chi^q(G)$ with the same possibilities for q or $\text{length}(\mathcal{S}) = \chi_{\text{int}}^{q^*}(G)$.

While the combined requirements involve the exact solution of NP-hard problems (finding any of $\chi(G)$, $\chi_{\text{int}}^*(G)$, and $\chi^*(G)$ is NP-hard; cf., respectively, [17], [7], and [14]), the former one alone is always a property of schedules based on multicolorings when buffering availability is unbounded. To see that this is so, first recall that the definition of $\text{delivered}(\mathcal{S})$ refers to a repetition of the whole schedule as far down in time as needed for any transient effects to have waned. So, given any of the P source-to-destination paths, we can prove that $\text{delivered}(\mathcal{S}) = Pq$ by arguing inductively about what happens on such a path during that future repetition of \mathcal{S} . The basis case in this induction is the first directed edge on the path (the one leading out of the source). The property that every appearance of this edge does indeed transmit a packet follows trivially from the fact that the source has an endless supply of new packets to provide whenever needed. Assuming that this also happens to the next-to-last edge on the path (this is our induction hypothesis) immediately leads to the same conclusion regarding the last edge, the one on which $\text{delivered}(\mathcal{S})$ is defined. To see this, let e be the last edge and e^- the next-to-last one. Because \mathcal{S} is repeated indefinitely, every time slot t sufficiently far down in time in which e appears is the closing time slot of a window in which both e and e^- appear exactly q times each. By the induction hypothesis, it follows that at least one packet is guaranteed to exist for transmission through e at time slot t .

Buffering availability, however, is not unbounded, so we must argue for its finiteness. We do this by recognizing another important property of multicoloring-based schedules, one that is related to constraints C1 and C2 introduced earlier. Because every edge of D (node of G) appears the exact same number q of times

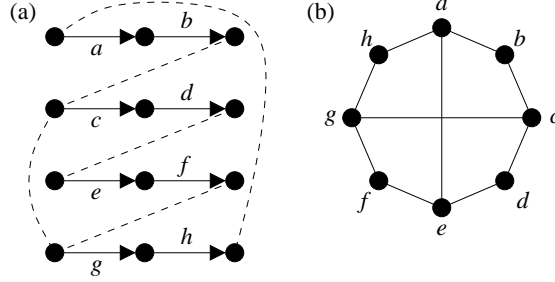


Figure 4: A set of $P = 4$ paths (a), with dashed lines indicating all node pairs representing off-path interference. The resulting graph G is shown in panel (b). Depending on the schedule \mathcal{S} it is possible to obtain equalities in all of Eqs. (3)–(5). The schedules that achieve this while implying strict inequalities in Eq. (6) are: $\mathcal{S} = \langle \{a, d, g\}, \{b, f, h\}, \{c, e\} \rangle$ for Eq. (3), with $T^1(\mathcal{S}) = 4/3 \approx 1.33$; $\mathcal{S} = \langle \{a, d, f\}, \{b, e, g\}, \{c, f, h\}, \{a, d, g\}, \{b, e, h\}, \{a, c, f\}, \{b, d, g\}, \{c, e, h\} \rangle$ for Eq. (5), with $T_{\text{int}}^*(\mathcal{S}) = 4/(8/3) = 1.5$; and $\mathcal{S} = \langle \{a, c, f\}, \{b, e, g\}, \{c, e, h\}, \{a, d, g\}, \{b, d, f, h\} \rangle$ for Eq. (4), with $T^*(\mathcal{S}) = 4/(5/2) = 1.6$.

in \mathcal{S} , there certainly always is a finite value of B , the number of buffer positions per node per path that goes through it, such that C1 and C2 are satisfied. In all interleaved cases, this value is $B = 1$.

An example illustrating all of this is presented in Figure 4, where we give a set of four source-to-destination paths, the graph G that eventually results from them, and also the three schedules that result in equalities in Eqs. (3)–(5). In this case the two inequalities in Eq. (6) are strict, since it can be shown that $\chi(G) = 3$, $\chi_{\text{int}}^*(G) = 8/3$, and $\chi^*(G) = 5/2$ [26, 7].

5 Scheduling by edge reversal

From the three schedules illustrated in Figure 4 it would seem that finding a schedule \mathcal{S} to maximize $T(\mathcal{S})$ requires that we give up on the interleaved character of the underlying multicoloring and, along with it, give up on the equivalent property that edges of D that are consecutive on some source-to-destination path appear in \mathcal{S} alternately. However, once color interleaving is assumed we are automatically provided with a principled way to heuristically try and maximize $T(\mathcal{S})$ by appealing to a curious relationship that exists between multicolorings and the acyclic orientations of G . We now review this heuristic and later build on it by showing how to adapt it to abandon interleaving only on occasion during a schedule, aiming at maximizing $T(\mathcal{S})$.

An orientation of G is an assignment of directions to its edges. An orientation of G is acyclic if no directed cycles are formed. Every acyclic orientation has a set of sinks (nodes with no edges oriented outward), which by definition are not neighbors of one another. An acyclic orientation's set of sinks is then an

independent set. The heuristic we now describe, known as scheduling by edge reversal (SER) [7, 5], is based on the following property. Should an acyclic orientation be transformed into another by turning all its sinks into sources (nodes with no edges oriented inward), and should this be repeated indefinitely, we would obtain an infinite sequence of independent sets, each given by the set of sinks of the current orientation. Though infinite, this sequence must necessarily reach a point from which a certain number of acyclic orientations gets repeated indefinitely. This follows from the facts that there are only finitely many acyclic orientations of G and that turning one of them into the next is a deterministic process.

The orientations that participate in this cyclic repetition, henceforth called a period, have the property that every node of G appears as a sink in the same number of orientations. Furthermore, any two neighboring nodes of G are sinks in alternating orientations, regardless of whether the period has already been reached or not. It clearly follows that the sets of sinks in a period constitute a schedule that is based on an interleaved multicoloring. Depending on the very first acyclic orientation in the operation of SER more than one period can eventually be reached. The different periods' properties vary from one to another, but it can be shown that at least one of them corresponds to the optimal interleaved multicoloring, i.e., the one that yields $\chi_{\text{int}}^*(G)$ [7]. The heuristic nature of SER is then revealed by the need to determine an appropriate initial acyclic orientation.

Determining a schedule \mathcal{S} by SER follows the algorithm given next. We use $\omega_0, \omega_1, \dots$ to denote the sequence of acyclic orientations of G . For $t = 0, 1, \dots$, we denote by $\text{Sinks}(\omega_t)$ the set of sinks of ω_t .

ALGORITHM SER:

1. Choose ω_0 .
2. $t := 0$.
3. Obtain ω_{t+1} from ω_t .
4. If the period has not yet occurred, then $t := t + 1$; go to Step 3. If it has, then let $p(\omega_0)$ be its number of orientations, $m(\omega_0)$ the number of times any node appears in them as a sink, and $\omega_k, \omega_{k+1}, \dots, \omega_{k+p(\omega_0)-1}$ the orientations themselves. Output

$$\mathcal{S} = \langle \text{Sinks}(\omega_k), \text{Sinks}(\omega_{k+1}), \dots, \text{Sinks}(\omega_{k+p(\omega_0)-1}) \rangle$$

and

$$T(\mathcal{S}) = \frac{Pm(\omega_0)}{p(\omega_0)}.$$

In this algorithm, the explicit dependency of both $p(\omega_0)$ and $m(\omega_0)$ on ω_0 is meant to emphasize that, implicitly, the two quantities are already determined when in Step 1 the initial orientation ω_0 is chosen. As with the very existence of

the period, this follows from the fact that the algorithm's Step 3 is deterministic, so there really is no choice regarding the period to be reached once ω_0 has been fixed. The role played by the two quantities is precisely to characterize the interleaved multicoloring mentioned above. That is, the period reached from ω_0 can be regarded as assigning $q = m(\omega_0)$ distinct colors to each node of G using a total number $p = p(\omega_0)$ of colors. Equivalently, it can be regarded as a schedule \mathcal{S} for which $\text{delivered}(\mathcal{S}) = Pq = Pm(\omega_0)$ (where the first equality is true of all multicoloring-based schedules, as we discussed in Section 4) and $\text{length}(\mathcal{S}) = L = p = p(\omega_0)$. By Eq. (1), the final determination of $T(\mathcal{S})$ follows easily.

As a final observation, we note that, although the knowledge of $p(\omega_0)$ and $m(\omega_0)$ after Step 1 is only implicit, it can be shown that the ratio $m(\omega_0)/p(\omega_0)$ can be known explicitly at that point [7]. It might then seem that the remainder of the algorithm is useless, since the value of $T(\mathcal{S})$ can be calculated right after Step 1. But the reason why the remaining steps are needed, of course, is that \mathcal{S} itself needs to be found, not just the $T(\mathcal{S})$ that quantifies its performance.

6 Improving on SER

In Figure 5 we provide an example to illustrate why giving up interleaving may yield a schedule \mathcal{S} of higher $T(\mathcal{S})$. The general idea is that, given B , it may be possible to schedule a given transmission sooner than it normally would be scheduled by SER, provided there is a packet to be transmitted in the buffers of the sending node in D and the receiving node has an available buffer position for the path in question. While under SER two transmissions sharing a buffer alternate with each other in any schedule (and then $B = 1$ always suffices), disrupting this alternance implies that all buffering is to be managed in detail.

In the example of Figure 5 transmissions g , h , and i are scheduled without regard to alternance if $B = 2$. While this results in improved performance (more packets delivered to node 4 per time slot), it is important to realize that this is in great part made possible by the structure of D in this example. Even though all three paths lead from node 1 to node 4, two of them are poised to interfere with each other particularly heavily by virtue of sharing node 2. The consequence of this is that transmissions on these paths will occur less in parallel than they might otherwise. But since $B = 2$ buffering positions are available per node per path, the path that goes through nodes 6 and 7 can compensate for this by transmitting twice as much traffic (thence the double occurrence of g in a row, and also of h and i , for each repetition of the schedule). This, however, is never detrimental to the traffic on the other two paths: all that is being done is to seize the opportunity to transmit in time slots that would otherwise go unused.

Implementing the careful buffer management alluded to above requires that we look at the dynamics of acyclic-orientation transformation under SER in more detail. Given any acyclic orientation ω of G , the node set N of G can be partitioned into independent sets I_1, I_2, \dots, I_d such that I_1 is the set of all sinks in G according to ω , I_2 is the set of all sinks we would obtain if all

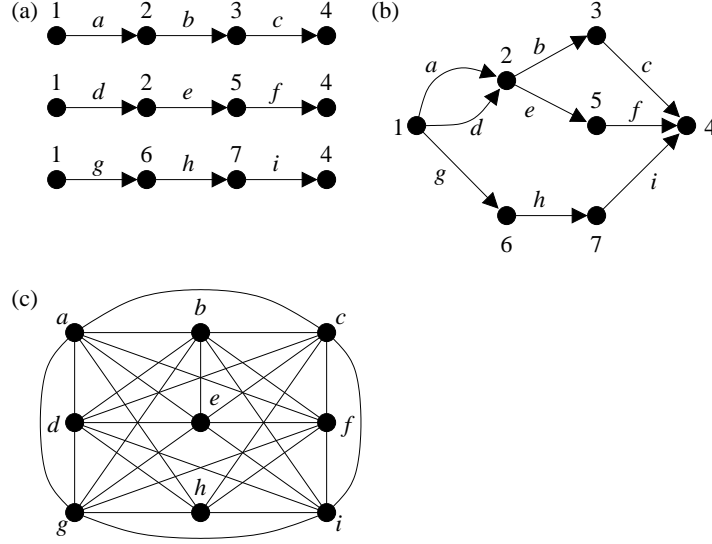


Figure 5: A set of $P = 3$ directed paths (a), the resulting directed multigraph D (b), and the resulting undirected graph G (c). The optimal SER schedule is $\mathcal{S} = \langle \{a\}, \{b\}, \{c, g\}, \{d, i\}, \{e, h\}, \{f\} \rangle$, yielding $T(\mathcal{S}) = 3/6 = 0.5$. An alternative schedule that does not comply with the SER alternance condition, with $B = 2$, is $\mathcal{S} = \langle \{g, c\}, \{g, f\}, \{h, b\}, \{h, e\}, \{i, a\}, \{i, d\} \rangle$, which results in an improvement to $T(\mathcal{S}) = 4/6 \approx 0.67$.

nodes in I_1 were to be eliminated, and so on. In this partition, known as a sink decomposition, d is the number of nodes on a longest directed path of G according to ω . When ω is turned into ω' by SER a new sink decomposition is obtained, call it $I'_1, I'_2, \dots, I'_{d'}$, such that $I'_1 = I_2, I'_2 \supseteq I_3$, etc., with $d' \leq d$. The reason why equality need not hold in all cases, but set containment instead, is that each I_k may get enlarged by some of the previous orientation's sinks before becoming I'_{k-1} .

It is then possible to regard the operation of SER as simply a recipe for manipulating sink decompositions. At each iteration the set containing the current sinks is eliminated and its nodes are redistributed through the other sets. The remaining sets are renumbered by decrementing their subscripts by 1 and a new, greatest-subscript set may have to be created. The rule for redistributing each of the former sinks is to find the set of greatest subscript containing one of the node's neighbors in G , say I_k , and then place the node in set I_{k+1} . This is illustrated in panels (a) and (b) of Figure 6.

Altering this rule is the core of our modified SER, henceforth called SER with advancement (SERA). If i is the sink in question, the operation of SERA is based on placing node i in the least-subscript set that does not contain a neighbor of i in G . This clearly maintains acyclicity just as the previous rule does, but now the former sink is not necessarily turned into a source, but rather

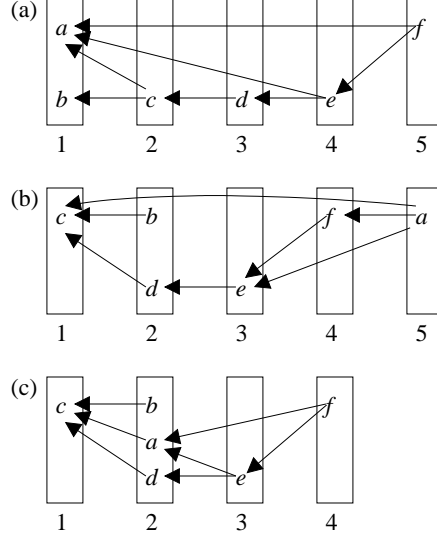


Figure 6: Each set in a sink decomposition is represented by a rectangular box and numbered to indicate the set's subscript. Note that directed edges refer to acyclic orientations of G . Applying SER to the sink decomposition in panel (a) yields the one in panel (b). In this transformation both a and b are turned into sources. The alternative of using SERA, on the other hand, makes it possible for a to be placed in a lower-subscript set, avoiding the transformation into a source and yielding the sink decomposition in panel (c). This can be done only because the set to which a is added contains none of its neighbors in G . Assuming that transmissions a , e , and f are initially arranged consecutively in one of the P paths in the order e, a, f , we have $i^- = e$, $i = a$, and $i^+ = f$. We also have, in reference to panel (a), $k^- = 4$, $k = 2$, and $k^+ = 5$. Then the additional conditions for the move from (a) to (c) to occur are that the buffers shared by transmissions e and a contain at least one packet (since $k < k^-$), and that those shared by a and f have room for at least one packet (since $k < k^+$).

into a node that can have edges oriented both inward and outward by the current orientation, respectively from nodes in sets of greater subscripts and to nodes in sets of lesser subscripts. Additionally, while this alternative placement of node i does favor it by virtue of lowering the number of time slots that need to go by before it is a sink once again, clearly there is no detriment to any of the other transmissions, which will assuredly become sinks no later than they would otherwise.

As we mentioned, however, unlike SER this rule can only be applied as a function of B and the buffering-related constraints we mentioned. Suppose that i is preceded by transmission i^- and succeeded by transmission i^+ on the original path out of $\mathcal{P}_1, \mathcal{P}_2, \dots, \mathcal{P}_P$ to which it belongs. Of course, both i^- and i^+ are nodes of G as well. Suppose further that these two nodes are in

sets I_{k^-} and I_{k^+} , respectively, and that we are attempting to place node i in set I_k . The further constraints to be satisfied are the following. If $k < k^-$, then the buffers shared by transmissions i^- and i must contain at least one packet to be transmitted. If $k < k^+$, then the buffers shared by transmissions i and i^+ must contain room to store at least one more packet. This can all be implemented rather easily by keeping a dynamic record of all buffers. A simple case of evolving sink decompositions in the SERA style is shown in panels (a) and (c) of Figure 6.

SERA, like SER, operates on finitely many possibilities and deterministically. A “possibility” is no longer simply an acyclic orientation, but instead an acyclic orientation together with a configuration of buffer occupation. In any event, periodic behavior is still guaranteed to occur and we go on denoting by $p(\omega_0)$ the number of possibilities in the period that one reaches from ω_0 . The notion behind $m(\omega_0)$, however, has been lost together with the certainty of interleaving, since SERA does not guarantee that every node of G is a sink in the period the same number of times. For $i \in N$, an alternative definition is that of $m_i(\omega_0)$, which we henceforth use to denote the number of times node i is a sink in the period, not necessarily the same for all nodes.

Determining the schedule \mathcal{S} through SERA proceeds according to the following algorithm.

ALGORITHM SERA:

1. Choose ω_0 .
2. $t := 0$.
3. Obtain ω_{t+1} from ω_t , employing advancement as described.
4. If the period has not yet occurred, then $t := t + 1$; go to Step 3. If it has, then let $p(\omega_0)$ be its number of orientations (with associated buffer-occupation configurations), $m_i(\omega_0)$ the number of times node i appears in them as a sink, and $\omega_k, \omega_{k+1}, \dots, \omega_{k+p(\omega_0)-1}$ the orientations themselves. Output

$$\mathcal{S} = \langle \text{Sinks}(\omega_k), \text{Sinks}(\omega_{k+1}), \dots, \text{Sinks}(\omega_{k+p(\omega_0)-1}) \rangle$$

and

$$T(\mathcal{S}) = \frac{\sum_{i \in T} m_i(\omega_0)}{p(\omega_0)},$$

where T is the set of the nodes of G that correspond to terminal edges of the paths $\mathcal{P}_1, \mathcal{P}_2, \dots, \mathcal{P}_P$.

In this algorithm, note that the determination of $T(\mathcal{S})$ generalizes what is done in SER. This is achieved by adopting $\text{delivered}(\mathcal{S}) = \sum_{i \in T} m_i(\omega_0)$ while maintaining $\text{length}(\mathcal{S}) = p(\omega_0)$ in Eq. (1). Particularizing this to the case of SER yields $\text{delivered}(\mathcal{S}) = Pm(\omega_0)$, as desired, since $m_i(\omega_0)$ becomes $m(\omega_0)$ for any node i of G and moreover $|T| = P$.

7 Methods

We have conducted extensive computational experiments to evaluate SER and SERA, the latter with a few different values for the buffering parameter B . Before we present results in Section 8, here we pause to introduce the methodology that was followed. This includes selecting the network topology that eventually leads to graph G and the choice of the initial acyclic orientation of G .

7.1 Topology generation

We generated 1600 networks by placing n nodes inside a square of side 1500. For each network the first node was positioned at the square's center. Given the nodes' communication (or interference) radius R , and with it the neighborhood relation among nodes (i.e., two nodes are neighbors of each other if and only if the Euclidean distance between them is no greater than R), we proceeded to positioning the remaining nodes randomly, one at a time. Positioning a node was subject to the constraints that it would have at least one neighbor, that no node would have more than Δ neighbors, and moreover that no two nodes would be closer to each other than 25 units of Euclidean distance. Repeated attempts at positioning nodes while satisfying these constraints were not allowed to number more than 1000 per network. When this limit was reached the growing network was wiped clean and a new one was started. The value of R was determined so that, had the nodes been positioned uniformly at random, a randomly chosen radius- R circle would have expected density proportional to Δ/R^2 and about the same density as the whole network, i.e., $\Delta/R^2 \propto n$. Choosing the proportionality constant to yield $R = 200$ for $n = 80$ and $\Delta = 4$ results in the formula $R = 200\sqrt{20\Delta/n}$. Of the 1600 networks thus generated, there are 100 networks for each combination of $n \in \{60, 80, 100, 120\}$ and $\Delta \in \{4, 8, 16, 32\}$.

For each network we generated $50n$ sets of paths $\mathcal{P}_1, \mathcal{P}_2, \dots, \mathcal{P}_P$, each 100 sets corresponding to a different value of P . Each of the sets resulted in a different D , then in G , as explained in Sections 2 and 3. The $50n$ sets comprise 100 groups of $n/2$ sets each. The first of these sets for a group has $P = 1$ and the single path it contains is the shortest path from a randomly chosen node to another in the network. Each new set in the group is the previous one enlarged by the addition of a new path, obtained by selecting two distinct nodes randomly, provided they do not already participate in the previous set. This goes on until $P = n/2$, so in the last set every one of the n nodes participates as either the origin or the destination of one of the P paths. For the sake of normalization, the results we present for $T(\mathcal{S})$, given for $P = 1, 2, \dots, n/2$, are shown against the ratio $P' = 2P/n \in (0, 1]$.

7.2 Initial acyclic orientation

Once G has been built for a fixed network and a fixed set of paths, the acyclic orientation ω_0 of G has to be determined. Our general approach is to label

every node of G with a different number and then to direct each edge from the node that has the higher number to the one that has the lower. Although the resulting orientation is clearly acyclic, we are left with the problem of labeling the nodes. We approach this problem by resorting to the paths $\mathcal{P}_1, \mathcal{P}_2, \dots, \mathcal{P}_P$ from which G resulted, since the nodes of G are in one-to-one correspondence with the directed edges on the paths. It then suffices to number the paths' edges.

We consider four numbering schemes:

ND-BF. The paths are organized in the nondecreasing order of their numbers of edges (ties are broken by increasing path number). The edges are then numbered breadth-first from the path's origins, given this organization of the paths.

ND-DF. The paths are organized in the nondecreasing order of their numbers of edges (ties are broken by increasing path number). The edges are then numbered depth-first from the paths' origins, given this organization of the paths.

NI-BF. The paths are organized in the nonincreasing order of their numbers of edges (ties are broken by increasing path number). The edges are then numbered breadth-first from the paths' origins, given this organization of the paths.

NI-DF. The paths are organized in the nonincreasing order of their numbers of edges (ties are broken by increasing path number). The edges are then numbered depth-first from the paths' origins, given this organization of the paths.

8 Computational results

We divide our results into two categories. First we give statistics on the 1600 networks generated for evaluation of the algorithms. Then we report on the values obtained for $T(\mathcal{S})$ by SER and SERA.

One of the statistics is particularly useful: despite its simplicity, we have found it to correlate with the SERA results in a fairly direct way. This statistic is based on a function of G that aims to quantify how the interference among the initial P directed paths is reflected in the structure of G . We denote this function by $\rho(G)$ and let it be such that

$$\rho(G) = \frac{P|E'|}{\sum_{p=1}^P |Y_p|}. \quad (8)$$

In this equation, recall that the sets Y_1, Y_2, \dots, Y_P , one for each of the initial directed paths, contain the edges that ultimately become the nodes of G . Thus, $\sum_{p=1}^P |Y_p|/P$ is the average number of edges on a path. Moreover, we let $E' \subseteq E$ be the set of G 's edges whose end nodes correspond to edges of distinct paths. In

words, then, $\rho(G)$ is the average number of off-path transmissions that interfere with the transmissions of a path having the average number of edges.

8.1 Properties of the networks generated

The 1600 networks' distributions of node degrees are given in Figure 7, which contains one panel for each of the four values of Δ and all four values of n . Their distributions of the numbers of edges on the P paths for $P = n/2$ are given in Figure 8, again with one panel for each of the four values of Δ and all four values of n .

We see from Figure 7 that the degree distributions peak at the degree Δ , falling approximately linearly toward the lower degrees (except for $\Delta = 32$, where a plateau is observed midway). Furthermore, the lowest observed degree grows with Δ , which is expected from the formula that gives the radius R as an increasing function of Δ . We also see from the figure that these distributions are approximately independent of the value of n for fixed Δ ; in reference to that same formula, we see that letting R decrease with n does indeed have the expected effect of maintaining an approximately uniform node density throughout the containing square.

We also expect path sizes to be smaller as Δ increases, and this is in fact what Figure 8 shows. In fact, larger Δ values decreases the variability of path sizes, which moreover get concentrated around an ever smaller mean. For fixed Δ , what we see in the figure is a consistent shift to the right (i.e., greater path sizes) as n grows. This reflects the fact that larger n for fixed Δ leads to smaller R , thus to longer paths.

These observations are summarized in Table 1, where the mean degree and mean path size are given for each combination of n and Δ values. This table also shows the average value of $\rho(G)$, defined above as an indicator of how much interference there is in G among all P paths, when G refers to $P = n/2$. For fixed n , it is curious to observe that $\rho(G)$ decreases as Δ is decreased from 32 through 8, but then appears to flatten out or even rebound slightly as Δ is further decreased to 4. Each of these averages corresponds to 10^4 G instances (100 instances corresponding to the $P = n/2$ case of each of the 100 networks for fixed n and Δ) and is significant to the extent of the confidence interval reported for it in the table's rightmost column. As we demonstrate shortly, the peculiar behavior of $\rho(G)$ helps explain a lot of what is observed with respect to how $T(S)$ behaves in the case of SERA.

8.2 Results

Our results for SER are given in Figure 9 as plots of $T(S)$ against the P' ratio introduced in Section 7. Each of the figure's four panels is specific to a fixed Δ value and shows a plot for each value of n combined with either the ND-BF or the ND-DF numbering scheme. All results relating to the NI-BF and NI-DF schemes are omitted, as we found them to be statistically indistinguishable from their ND counterparts. From this figure it seems clear that, as P' increases

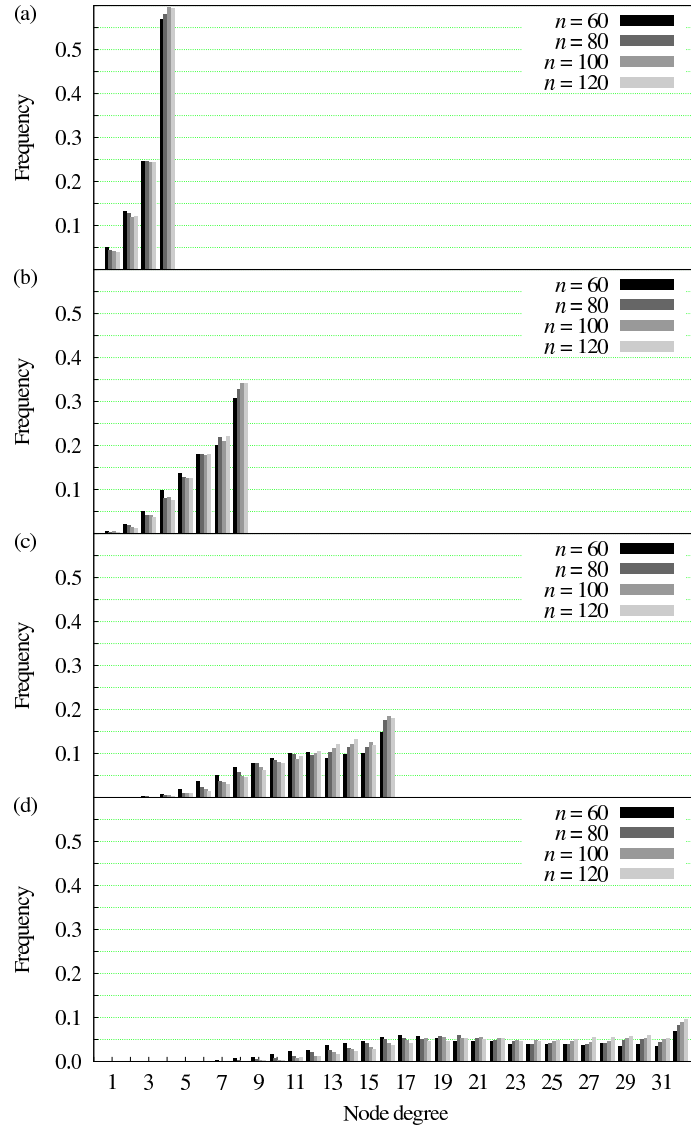


Figure 7: Degree distributions of the 1600 networks, for $\Delta = 4$ (a), $\Delta = 8$ (b), $\Delta = 16$ (c), and $\Delta = 32$ (d). For each combination of n and Δ the distribution refers to 100 networks.

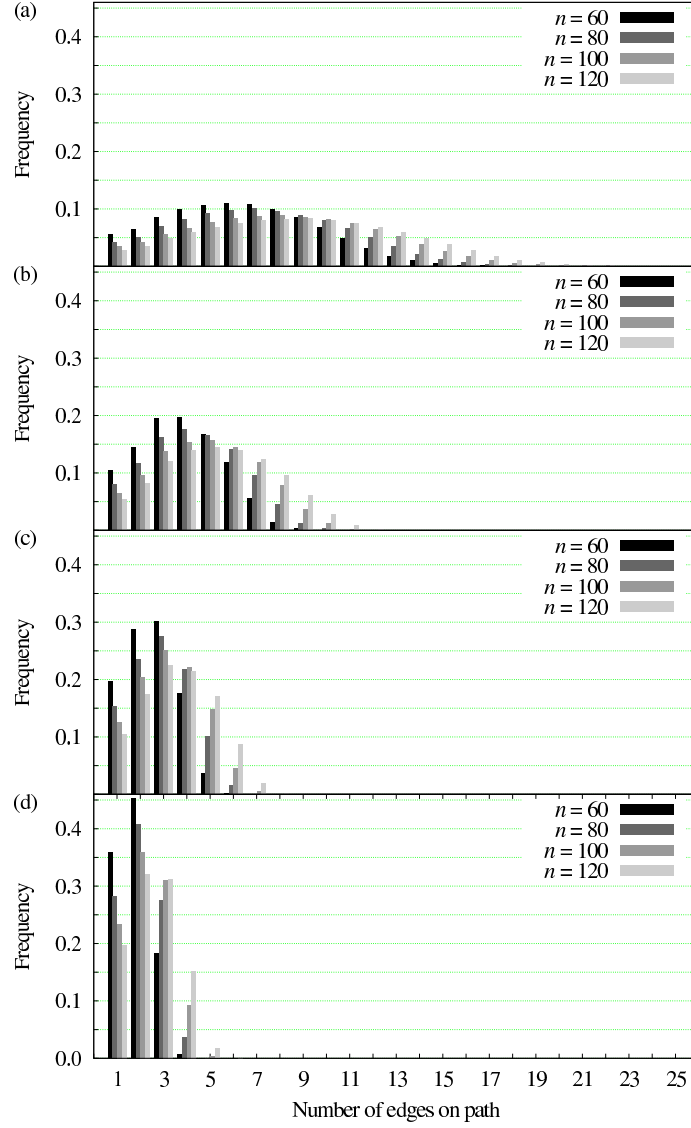


Figure 8: Path-size (number of edges) distributions of the 1600 networks, for $\Delta = 4$ (a), $\Delta = 8$ (b), $\Delta = 16$ (c), and $\Delta = 32$ (d). For each combination of n and Δ the distribution refers to 100 networks and to 100 path sets for each network, each set comprising $P = n/2$ paths.

Table 1: Mean values of the distributions in Figures 7 and 8, and the average $\rho(G)$ values for the 10^4 G instances corresponding to each combination of n and Δ when $P = n/2$. Confidence intervals refer to these averages and are given at the 95% level.

n	Δ	Mean degree	Mean path size	$\rho(G)$	
				Average	Conf. int.
60	4	3.33	7.46	0.4	0.06
	8	6.22	4.85	0.37	0.06
	16	11.67	3.57	0.4	0.05
	32	21.23	2.84	0.58	0.05
80	4	3.36	8.32	0.37	0.06
	8	6.37	5.36	0.35	0.06
	16	12.17	3.92	0.39	0.05
	32	22.36	3.06	0.59	0.05
100	4	3.40	9.3	0.36	0.06
	8	6.40	5.86	0.34	0.07
	16	12.40	4.22	0.38	0.06
	32	23.09	3.27	0.6	0.05
120	4	3.40	9.95	0.34	0.06
	8	6.45	6.28	0.33	0.07
	16	12.50	4.52	0.38	0.06
	32	23.59	3.47	0.58	0.05

(i.e., as the number of paths P grows towards $n/2$), the superiority of the BF schemes over the DF schemes becomes apparent, more pronouncedly so for the lower values of Δ . The reason why the BF schemes tend to perform better than the DF schemes should be intuitively clear: the BF schemes number the transmissions that are closer to the paths' origins first, therefore with the lowest numbers. As the initial acyclic orientation of G is built from these numbers, the first sinks during the operation of SER will correspond to starting parallel traffic on as many paths as possible. Overall it also seems that larger values of n lead to better performance for fixed Δ , but the distinction appears to be only marginal and is sometimes obscured by the confidence intervals.

A similar set of plots is given in Figure 10, now displaying our results for SERA as plots of $T(\mathcal{S})$ against the ratio P' . Once again there is one panel for each value of Δ , and once again several possibilities regarding the numbering schemes are omitted because of statistical indistinguishability. This is also true of the various possibilities for the value of B , with the single exception we mention shortly. Thus, most plots correspond to the ND-BF numbering scheme with $B = 1$. The single exception is that of $n = 60$ with $\Delta = 4$, for which we also report on the $B = 2$ case. For fixed Δ and P' , increasing n also leads to increased $T(\mathcal{S})$. In the particular case of $n = 60$ and $\Delta = 4$, increasing B from 1 to 2 also causes $T(\mathcal{S})$ to increase.

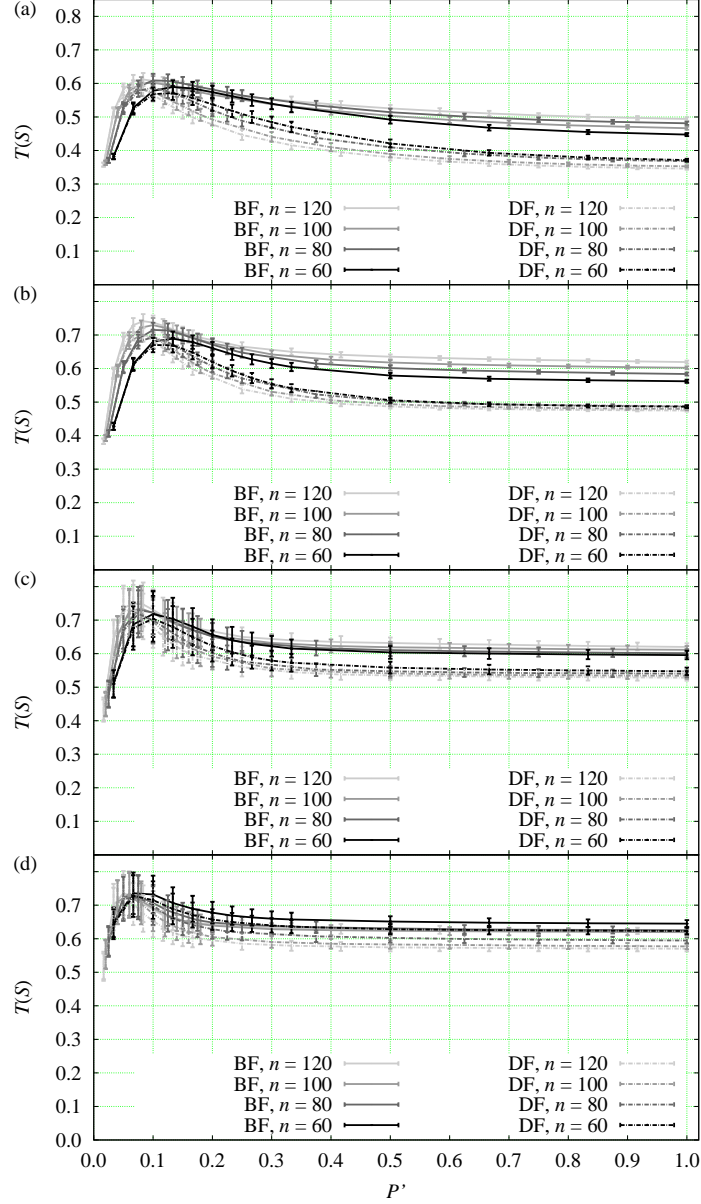


Figure 9: Behavior of $T(S)$ for SER under the two numbering schemes ND-BF and ND-DF, with $\Delta = 4$ (a), $\Delta = 8$ (b), $\Delta = 16$ (c), and $\Delta = 32$ (d). Data are averages over the 10^4 G instances that correspond to each combination of n and Δ for each value of P . Error bars are based on confidence intervals at the 95% level.

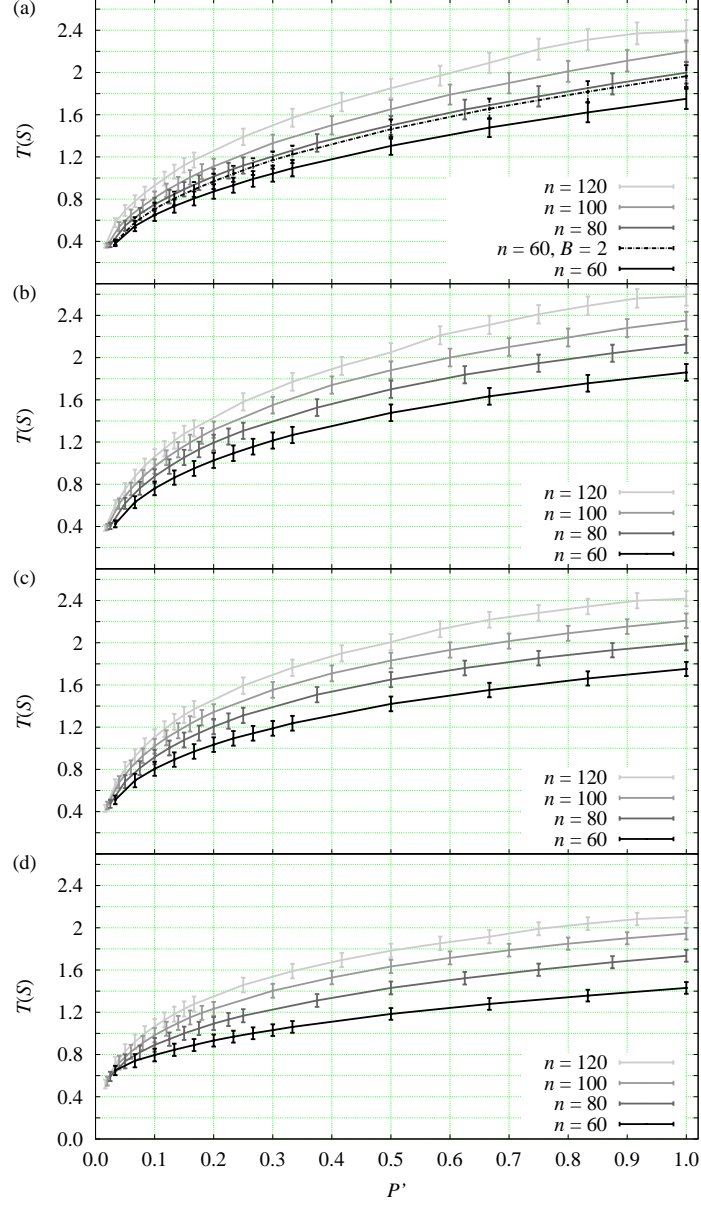


Figure 10: Behavior of $T(S)$ for SERA under the numbering scheme ND-BF, with $\Delta = 4$ (a), $\Delta = 8$ (b), $\Delta = 16$ (c), and $\Delta = 32$ (d). Data are averages over the 10^4 G instances that correspond to each combination of n and Δ for each value of P . Error bars are based on confidence intervals at the 95% level.

As we fix Δ , n , and P' , Figures 9 and 10 reveal that $T(\mathcal{S})$ is consistently higher for SERA than it is for SER (by a factor of about 2 to 4) across all values for these quantities, thereby establishing the superiority of the former algorithm over the latter. For sufficiently large n this occurs for the same value of B (that is, for $B = 1$), which furthermore establishes that this superiority does not in general depend on the availability of more buffering space. It is, instead, determined solely by the elimination in SERA of the mandatory alternance of interfering transmissions in SER.

Fixing n and P' while varying Δ (i.e., moving between panels) yields further interesting insight about the two algorithms. While for SER increasing Δ under these conditions causes $T(\mathcal{S})$ to increase monotonically (though sometimes almost imperceptibly) for the same numbering scheme, doing the same for SERA for constant B leads $T(\mathcal{S})$ to behave in a markedly non-monotonic way. In fact, as Δ is increased from 4 to 8 there is also an increase in $T(\mathcal{S})$, but increasing Δ further through $\Delta = 32$ leads to decreases in $T(\mathcal{S})$. As we anticipated earlier, this is fully analogous to the behavior of $\rho(G)$ as Δ is increased in the same way while all else remains constant. This suggests that what determines the relative behavior of $T(\mathcal{S})$ in these circumstances is the intensity of inter-path interference as it gets shaped by the structure of G . In other words, $T(\mathcal{S})$ and $\rho(G)$ tend to vary along somewhat inverse trends with respect to each other.

9 Discussion

When SER is used, it follows from our discussion in Sections 4 and 5 that $T(\mathcal{S}) = T_{\text{int}}^*(\mathcal{S})$. By Eq. (5), we then have

$$T(\mathcal{S}) \leq \frac{P}{\chi_{\text{int}}^*(G)}, \quad (9)$$

where achieving equality requires that we choose ω_0 optimally. Now let $\varphi(G) = \max\{\omega(G), |N|/\alpha(G)\}$, where $\omega(G)$ is the number of nodes in the largest clique of G and $\alpha(G)$ is the number of nodes in the largest independent set of G . It can be shown that $\chi_{\text{int}}^*(G) \geq \varphi(G)$,¹ whence

$$T(\mathcal{S}) \leq \frac{P}{\varphi(G)} = \frac{P'n}{2\varphi(G)}, \quad (10)$$

where we have taken into account the way we handle P in all our experiments. We see then that $T(\mathcal{S})$ is bounded from above by the fraction of $n/2$ given by $P'/\varphi(G)$. For fixed P' , this fraction tends to be small if the largest clique of G is large or its largest independent set is small, whichever is more influential on $\varphi(G)$. Either possibility bespeaks the presence of considerable interference among the transmissions represented by the $|N|$ nodes of G .

¹See [18], where the interleaved multichromatic number of G is referred to as G 's circular chromatic number, and references therein.

Of course, in general we have no practical way of knowing how close each ω_0 we choose is to being the optimal starting point for SER, nor of knowing how different $\chi_{\text{int}}^*(G)$ and $\varphi(G)$ are for the G instances we use. So the bound given in Eq. (10), located somewhere between $30P'/\varphi(G)$ and $60P'/\varphi(G)$ for our values of n , cannot be used as a guide to assessing how low the $T(\mathcal{S})$ values shown in Figure 9 really are. But the bound's sensitivity to growing interference in G does provide some guidance, since all plots in the figure become flat from about $P' = 0.3$, regardless of the value of n or the numbering scheme used. Perhaps every G corresponding to such values of P' share some structural property, like a very large clique or only very small independent sets, that renders the resulting values of $T(\mathcal{S})$ oblivious to all else.

As for SERA, since the schedules it produces depart from a strict characterization as multicolorings of G , no upper bounds on $T(\mathcal{S})$ are known to us. Nevertheless, a comparison with SER as provided by Figures 9 and 10 reveals that $T(\mathcal{S})$ for SERA surpasses $T(\mathcal{S})$ for SER by a substantial margin, and also that SERA is capable of finding ways to improve $T(\mathcal{S})$ somewhat even as P' grows. If our observation above regarding the structure of G as an inherent barrier to improving $T(\mathcal{S})$ as P' grows is true, then the barrier's effects under SERA are considerably attenuated. This, we believe, is to be attributed to SERA's aggressively opportunistic approach of abandoning the interleaving that is the hallmark of SER.

10 Concluding remarks

Algorithms SER and SERA are methods for link scheduling in WMNs. As such, and unlike other methods for link scheduling, they are built around a set of origin-to-destination paths and aim to provide as much throughput on these paths as possible. From a mathematical perspective they are both related to providing the nodes of a graph with an efficient multicoloring, in the sense discussed in Section 4. For SER this is strictly true, but for SERA the defining characteristic of a multicoloring, that each node receives the same number of colors, ceases to hold. As we demonstrated through our computational results in Section 8, it is precisely this deviation from the strict definition that allows SERA to surpass SER in terms of performance.

The functioning of both SER and SERA is supported by the use of the integer parameter $B \geq 1$, which indicates how many buffering positions each WMN node has to store in-transit packets for each of the paths that go through it. Choosing $B = 1$ suffices for SER because of its inherent property of alternating interfering transmissions, but $B > 1$ may in principle be needed for the advantages of SERA to become manifest. In the simulations we conducted, however, only rarely has this been the case, since on average increasing B beyond 1 provided no distinguishable improvement. In this regard, we find it important for the reader to refer to Figure 5 once again. As we remarked upon discussing that figure, profiting from a $B > 1$ situation under SERA is largely a matter of how uniformly interference gets distributed on the particular set of paths at hand.

Our results in Section 8, therefore, can safely be assumed to have stemmed from circumstances that, on average, led to highly uniformly distributed interference patterns.

The centerpiece of both SER and SERA is the undirected graph G , which embodies a representation of all the interference affecting the various wireless links represented by the graph's nodes. As we explained in Section 3, the steps to building G depend on how one assumes the communication and interference radii to relate to each other, and also on which interference model is adopted. We have given results for a specific set of assumptions, but clearly there is nothing in either method precluding its use under any other assumptions: all that needs to be done is construct G accordingly.

Analyzing either method mathematically is a difficult enterprise, but since their performance depends on the heuristic choice of an initial acyclic orientation of G , any effort profitably spent in that direction will be welcome. In addition to potentially better decisions regarding initial conditions, further mathematical knowledge on SER or SERA may also come to provide a deeper understanding of how upper bounds on $T(\mathcal{S})$ relate to what is observed. As we mentioned in Section 9, one such bound is already known in the case of SER. Obtaining better bounds in this case, as well as some bound in the case of SERA, remains open to further research.

Another issue that is open to further investigation is how to handle the potential difficulties that SER may encounter in the face of a growing number of nodes in G [20, 19]. These difficulties refer to the fact that, in the worst case, the time required to detect the occurrence of the period may grow exponentially with the square root of the number of nodes. They are inherited by SERA, since it generalizes SER, and may require the development of further heuristics if they pose a real problem in practice. In a related vein, sometimes it may be the case that only the value of $T(\mathcal{S})$ is needed, not \mathcal{S} itself. Knowing the achievable throughput without requiring knowledge of the schedule itself can be useful for evaluating WMN topologies or routing algorithms for them.

Should this be the case, then it is possible to estimate $T(\mathcal{S})$ more efficiently than using the full-fledged algorithms we gave. We can do this in the case of SERA by recognizing that $T(\mathcal{S})$ is the limit, as $t \rightarrow \infty$, of

$$T_t(\mathcal{S}) = \frac{\sum_{i \in T} m_i(\omega_0, t)}{t + 1}, \quad (11)$$

where $m_i(\omega_0, t)$ is the total number of times node i appears as a sink in orientations $\omega_0, \omega_1, \dots, \omega_t$. To see this, let $o(t)$ denote any function of t such that $\lim_{t \rightarrow \infty} o(t)/t = 0$. We then have $\sum_{i \in T} m_i(\omega_0, t) = r(t) \sum_{i \in T} m_i(\omega_0) + o(t)$ and $t + 1 = r(t)p(\omega_0) + o(t)$, where $r(t)$ is the number of times the period has been repeated up to iteration t . The limit follows easily, and automatically holds also for SER by straightforward extension. The streamlined version of either algorithm consists simply of letting t evolve either through a sufficiently large value determined beforehand or until $T_t(\mathcal{S})$ becomes stable. Any of the two alternatives does away with the need to detect the occurrence of the period.

We note, finally, that we have found the results given in Figure 10 to be practically indistinguishable from those obtained through the strategy outlined above for the computation of $T(\mathcal{S})$. We have verified this by letting $T(\mathcal{S}) = T_{t^+}(\mathcal{S})$, where t^+ is the least value of t for which $|T_t(\mathcal{S}) - T_{t-w}(\mathcal{S})|/T_{t-w}(\mathcal{S}) \leq 0.001$. Here w is a window parameter and in our experiments we used $w = |N|$. As for this particular choice, it comes from realizing that in both SER and SERA it takes at most $|N| - 1$ iterations for a node of G that is currently not a sink to become one. This, in turn, comes from the fact that in each iteration either algorithm necessarily decreases by 1 the number of edges on a longest directed path from any non-sink node to a sink. We can see that this is true of SER by viewing its dynamics in terms of how the orientations' sink decompositions evolve. We can see that it continues to hold in the case of SERA because SERA never places a former sink i into one of the sink-decomposition sets that already contains a neighbor of i in G (cf. Figure 6).

Acknowledgments

We acknowledge partial support from CNPq, CAPES, a FAPERJ BBP grant, and a scholarship grant from Université Pierre et Marie Curie. All computational experiments were carried out on the Grid'5000 experimental testbed, which is being developed under the INRIA ALADDIN development action with support from CNRS, RENATER, and several universities as well as other funding bodies (see <https://www.grid5000.fr>).

References

- [1] I. F. Akyildiz, X. Wang, and W. Wang. Wireless mesh networks: a survey. *Comput. Netw.*, 47:445–487, 2005.
- [2] M. Alicherry, R. Bhatia, and L. Li. Joint channel assignment and routing for throughput optimization in multi-radio wireless mesh networks. In *Proceedings of MobiCom 2005*, pages 58–72, 2005.
- [3] A. Balachandran, G. M. Voelker, and P. Bahl. Wireless hotspots: current challenges and future directions. *Mobile Netw. Appl.*, 10:265–274, 2005.
- [4] H. Balakrishnan, C. L. Barrett, V. S. A. Kumar, M. V. Marathe, and S. Thite. The distance-2 matching problem and its relationship to the mac-layer capacity of ad hoc wireless networks. *IEEE J. Sel. Area Commun.*, 22:1069–1079, 2004.
- [5] V. C. Barbosa. *An Introduction to Distributed Algorithms*. The MIT Press, Cambridge, MA, 1996.
- [6] V. C. Barbosa. The interleaved multichromatic number of a graph. *Ann. Comb.*, 6:249–256, 2000.

- [7] V. C. Barbosa and E. Gafni. Concurrency in heavily loaded neighborhood-constrained systems. *ACM Trans. Program. Lang. Syst.*, 11:562–584, 1989.
- [8] A. Behzad and I. Rubin. On the performance of graph-based scheduling algorithms for packet radio networks. In *Proceedings of IEEE GLOBECOM 2003*, pages 3432–3436, 2003.
- [9] J. A. Bondy and U. S. R. Murty. *Graph Theory*. Springer, New York, NY, 2008.
- [10] R. L. Cruz and A. V. Santhanam. Optimal routing, link scheduling and power control in multihop wireless networks. In *Proceedings of IEEE INFOCOM 2003*, pages 702–711, 2003.
- [11] I. Demirkol, C. Ersoy, and F. Alagoz. MAC protocols for wireless sensor networks: a survey. *IEEE Commun. Mag.*, 44(4):115–121, 2006.
- [12] S. Gandham, M. Dawande, and R. Prakash. Link scheduling in wireless sensor networks: distributed edge-coloring revisited. *J. Parallel Distrib. Comput.*, 68:1122–1134, 2008.
- [13] O. Goussevskaia, R. Wattenhofer, M. M. Halldorsson, and E. Welzl. Capacity of arbitrary wireless networks. In *Proceedings of IEEE INFOCOM 2009*, pages 1872–1880, 2009.
- [14] M. Grötschel, L. Lovász, and A. Schrijver. The ellipsoid method and its consequences in combinatorial optimization. *Combinatorica*, 1:169–197, 1981.
- [15] P. Gupta and P. R. Kumar. The capacity of wireless networks. *IEEE Trans. Inf. Theory*, 46:388–404, 2000.
- [16] Q.-S. Hua and F. C. M. Lau. Exact and approximate link scheduling algorithms under the physical interference model. In *Proceedings of DIAL M-POMC 2008*, pages 45–54, 2008.
- [17] R. M. Karp. Reducibility among combinatorial problems. In R. E. Miller and J. W. Thatcher, editors, *Complexity of Computer Computations*, pages 85–103. Plenum Press, New York, NY, 1972.
- [18] W. Lin. Some star extremal circulant graphs. *Discrete Math.*, 271:169–177, 2003.
- [19] Y. Malka, S. Moran, and S. Zaks. A lower bound on the period length of a distributed scheduler. *Algorithmica*, 10:383–398, 1993.
- [20] Y. Malka and S. Rajsbaum. Analysis of distributed algorithms based on recurrence relations. In *Distributed Algorithms*, volume 579 of *Lecture Notes in Computer Science*, pages 242–253. Springer, Berlin, Germany, 1992.

- [21] T. Moscibroda, R. Wattenhofer, and A. Zollinger. Topology control meets SINR: the scheduling complexity of arbitrary topologies. In *Proceedings of MobiHoc 2006*, pages 310–321, 2006.
- [22] N. Nandiraju, D. Nandiraju, L. Santhanam, B. He, J. Wang, and D. P. Agrawal. Wireless mesh networks: current challenges and future directions of web-in-the-sky. *IEEE Wirel. Commun.*, 14(4):79–89, 2007.
- [23] P. Santi, R. Maheshwari, G. Resta, S. Das, and D. M. Blough. Wireless link scheduling under a graded SINR interference model. In *Proceedings of ACM FOWANC 2009*, pages 3–12, 2009.
- [24] Y. Shi, Y. T. Hou, J. Liu, and S. Kompella. How to correctly use the protocol interference model for multi-hop wireless networks. In *Proceedings of MobiHoc 2009*, pages 239–248, 2009.
- [25] M. Siekkinen, V. Goebel, T. Plagemann, K.-A. Skevik, M. Banfield, and I. Brusic. Beyond the future Internet—requirements of autonomic networking architectures to address long term future networking challenges. In *Proceedings of FTDCS 2007*, pages 89–98, 2007.
- [26] S. Stahl. n -tuple colorings and associated graphs. *J. Comb. Theory B*, 20:185–203, 1976.
- [27] J. Wang, P. Du, W. Jia, L. Huang, and H. Li. Joint bandwidth allocation, element assignment and scheduling for wireless mesh networks with MIMO links. *Comput. Commun.*, 31:1372–1384, 2008.
- [28] W. Wang, Y. Wang, X.-Y. Li, W.-Z. Song, and O. Frieder. Efficient interference-aware TDMA link scheduling for static wireless networks. In *Proceedings of MobiCom 2006*, pages 262–273, 2006.
- [29] X. Wang and J. J. Garcia-Luna-Aceves. Embracing interference in ad hoc networks using joint routing and scheduling with multiple packet reception. *Ad Hoc Netw.*, 7:460–471, 2009.
- [30] X. Xu and S. Tang. A constant approximation algorithm for link scheduling in arbitrary networks under physical interference model. In *Proceedings of ACM FOWANC 2009*, pages 13–20, 2009.
- [31] H.-G. Yeh and X. Zhu. Resource-sharing system scheduling and circular chromatic number. *Theor. Comput. Sci.*, 332:447–460, 2005.